Effect of Al_2O_3 Addition and WO_3 Modification on Catalytic Activity of NiO/Al_2O_3-TiO_2/WO_3 for Ethylene Dimerization

Young Il Pae[†] **and Jong Rack Sohn**[*]

Department of Applied Chemistry, Engineering College, Kyungpook National University, Daegu 702-701, Korea
[*]*E-mail: jrsohn@knu.ac.kr*
[†]*Department of Chemistry, University of Ulsan, Ulsan 680-746, Korea*
Received July 24, 2007

Strong solid acid catalysts, NiO/Al_2O_3-TiO_2/WO_3 for ethylene dimerization were prepared by the addition of Al_2O_3 and the modification with WO_3. The acid sites and acid strength were increased by the inductive effect of WO_3 species bonded to the surface of catalysts. The larger the dispersed WO_3 amount, the higher both the acidity and catalytic activity for ethylene dimerization. The addition of Al_2O_3 to TiO_2 up to 5 mol% enhanced acidity and catalytic activity gradually due to the interaction between Al_2O_3 and TiO_2 and consequent formation of Al-O-Ti bond.

Key Words : Al_2O_3 addition, WO_3 modification, Acidity, Ethylene dimerization

Introcuction

Heterogeneous catalysts for the dimerization and oligomerization of olefins, consisting mainly of nickel compounds supported on oxides, have been known for many years. A considerable number of papers have dealt with the problem of nickel-containing catalysts for ethylene dimerization.[1-11] One of the remarkable features of this catalyst system is its activity in relation to a series of *n*-olefins. In contrast to usual acid-type catalysts, nickel oxide on silica or silica-alumina shows a higher activity for a lower olefin dimerization, particularly for ethylene.[1-6,12] It has been suggested that the active site for dimerization is formed by an interaction of a low-valent nickel ion with an acid site.[9,13] In fact, nickel oxide, which is active for C_2H_4-C_2D_4 equilibration, acquires an activity for ethylene dimerization upon addition of nickel sulfate, which is known to be an acid.[14] A transition metal can also be supported on zeolite in the state of a cation or a finely dispersed metal. Transition metal ions like Ni^+ or Pd^+ can be active sites in catalytic reactions such as ethylene and propylene dimerization as well as acetylene cyclomerization.[15-17]

The previous papers from this laboratory have shown that NiO-TiO_2 and NiO-ZrO_2 modified with sulfate or tungstate ions are very active for ethylene dimerization.[6,18-20] High catalytic activities in the reactions were attributed to the enhanced acidic properties of the modified catalysts, which originated from the inductive effect of S=O or W=O bonds of the complex formed by the interaction of oxides with sulfate or tungstate ions. However, catalytic functions have been improved by loading additional components. Sulfated zirconia incorporating Fe and Mn has been shown to be highly active for butane isomerization, catalyzing the reaction even at room temperature.[21,22] The promotion in activity of catalyst has been confirmed by several other reseach group.[23-25] Coelho et al. have discovered that the addition of Ni to sulfated zirconia causes an activity enhancement comparable to that caused the addition of Fe and Mn.[26] It has been reported by several workers that the addition of platinum to zirconia modified by sulfate ions enhances catalytic activity in the skeletal isomerization of alkanes without deactivation when the reaction is carried out in the presence of hydrogen.[27-29] Recently, it has been found that a main group element Al can also promote the catalytic activity and stability of sulfated zirconia for *n*-butane isomerization and ethylene dimerization.[30-32]

The search for a more active catalyst is a never ending task. At the same time that increased catalytic activity is sought, an improvement in selectivity to the desired product is also required. Recently, some workers reported zirconia or titania-supported WO_3 as alternative materials in reactions requiring strong acid sites.[33-36] Several advantages of tungstate over sulfate as dopant include the facts that they do not suffer from dopant loss during thermal threatment and that they undergo significantly less deactivation during catalytic reaction.[36] It is known that for titania-supported catalyst its surface area and catalytic activity are decreasing under the severe reaction condition. To overcome these deficiencies, titania was added by Al_2O_3 and was modified with WO_3 by taking advantage of high acidity, high thermal stability, and high surface area of modified TiO_2. In this paper we report new catalyst systems prepared by adding Al_2O_3 to TiO_2 and modifying TiO_2 with WO_3 for ethylene dimerization.

Experimental

Catalyst preparation. The Al_2O_3-TiO_2 mixed oxide was prepared by a co-precipitation method using aqueous ammonia as the precipitation reagent. The coprecipitate of $Al(OH)_3$-$Ti(OH)_4$ was obtained by adding aqueous ammonia slowly into a mixed aqueous solution of titanium tetrachloride and aluminum nitrate (Junsei Chemical Co.) at room temperature with stirring until the pH of the mother liquor reached about 8. NiO/Al_2O_3-TiO_2 was prepared by adding aqueous ammonia slowly into a mixed solution of $NiCl_2$ solution and $Al(OH)_3$-$Ti(OH)_4$ with stirring until the pH of solution reached about 8. The catalysts containing various tungsten oxide contents were prepared by adding an aqueous solution of ammonium metatungstate[$(NH_4)_6$-$(H_2W_{12}O_{40})\cdot nH_2O$] to the NiO/$Al_2O_3$-$TiO_2$ powder followed by drying and calcining at high temperatures for 1.5 h in air. This series of catalysts are denoted by their weight percentage of NiO and WO_3. For example, 20NiO/5Al_2O_3-TiO_2/15WO_3 indicates the catalyst containing 20 wt% NiO, and 15 wt% WO_3, and 5 mol% Al_2O_3 regarding only TiO_2.

Procedure. FTIR spectra were obtained in a heatable gas cell at room temperature using a Mattson Model GL6030E spectrophotometer. The self-supporting catalyst wafers contained about 9 mg cm^{-2}. Prior to obtaining the spectra, we heated each sample under vacuum at 100-400 °C for 1 h. Catalysts were checked in order to determine the structure of the prepared catalysts by means of a Philips X'pert-APD X-ray diffractometer, employing Ni-filtered Cu K_α radiation.

The specific surface area was determined by applying the BET method to the adsorption of N_2 at –196 °C. Chemisorption of ammonia was also employed as a measure of the acidity of catalysts. The amount of chemisorption was determined based on the irreversible adsorption of ammonia.[37-39]

The catalytic activity for ethylene dimerization was determined at 20 using a conventional static system following the pressure change from an initial pressure of 290 Torr. A fresh catalyst sample of 0.2 g was used for every run and the catalytic activity was calculated as the amount of ethylene consumed during initial 5 min. Reaction products were analyzed by gas chromatography with a VZ-7 column at room temperature.

Results and Discussion

Infrared spectra of WO_3 species. To examine the structure of tungsten oxide complex under dehydration conditions, infrared spectra of 20NiO/5Al_2O_3-TiO_2/15WO_3 samples were obtained in a heatable gas cell after evacuation at different temperatures for 1 h. The in situ infrared spectra in the 900-1100 cm^{-1} region for 20NiO/5Al_2O_3-TiO_2/15WO_3 are presented in Figure 1. The infrared single band at 1003-1012 cm^{-1} is due to the symmetrical W=O stretching mode of the tungsten oxide complex coordinated to the Al_2O_3-TiO_2 surface.[40] As shown in Figure 1, as evacuation temperature increases, the W=O stretching mode shifts upward from 1003 to 1012 cm^{-1}, the band becomes sharper, and the intensity increases. The similar results have been obtained with the other samples. This shows that the dehydration changes the molecular structures and that the two-dimensional tetrahedrally coordinated tungsten oxide species as well as the octahedrally coordinated polytungstate species are converted into the same highly distorted octahedrally coordinated structure as proposed for the WO_3/TiO_2 system by Wachs *et al.*[41] For the other 20NiO/5Al_2O_3-TiO_2/WO_3 samples containing different WO_3 contents and evacuated at 400 °C the band intensity at 1012 cm^{-1} increased with increasing the WO_3 content, indicating that the higher the WO_3 content, the more the octahedrally coordinated WO_3 species.

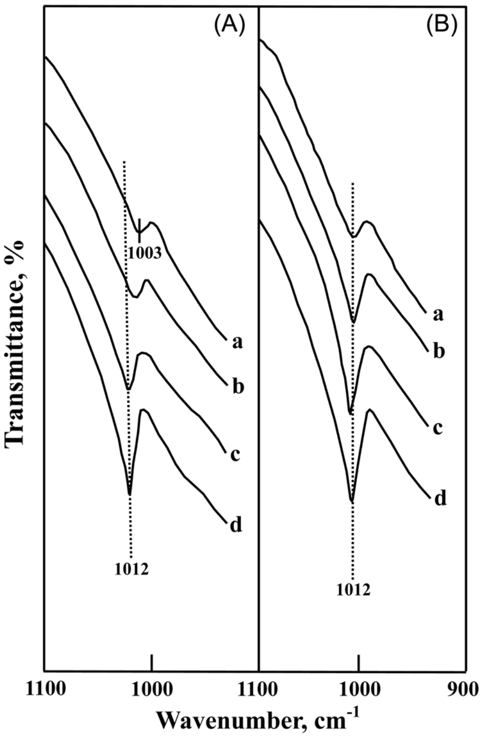

Figure 1. (A) Infrared spectra of 20NiO/5Al_2O_3-TiO_2/15WO_3 evacuated at different temperatures for 1 h: (a) 100 °C (b) 200 °C (c) 300 °C and (d) 400 °C. (B) Infrared spectra of 20NiO/5Al_2O_3-TiO_2/WO_3 containing different WO_3 contents and evacuated at 400 °C for 1 h: (a) 20NiO/5Al_2O_3-TiO_2/3WO_3 (b) 20NiO/5Al_2O_3-TiO_2/5WO_3 (c) 20NiO/5Al_2O_3-TiO_2/10WO_3 and (d) 20NiO/5Al_2O_3-TiO_2/15WO_3.

Crystalline structures of catalysts. The crystalline structures of catalysts calcined in air at different temperatures for 1.5 h were examined. In the case of titania support, as shown in Figure 2, TiO_2 was amorphous to X-ray diffraction at 25 °C, with an anatase phase 300-400 °C, a two-phase mixture of the anatase and rutile forms at 500-600 °C, and a rutile phase at 700-800 °C. Three crystal structures of TiO_2, *i.e.*, anatase, rutile, and brookite phases have been reported.[42,43] However, in the case of 5Al_2O_3-TiO_2, the crystalline structures of the samples were different from that of pure TiO_2. As shown in Figure 3, 5Al_2O_3-TiO_2 calcined at 400 °C are mostly amorphous. The transition temperature of TiO_2 from amorphous to anatase phase was higher by 200 °C than that of pure TiO_2. X-ray diffraction data indicated only the anatase phase of TiO_2 at 500-800 °C, showing that the amount of anatase TiO_2 phase increased with increasing the calcination temperature. It is assumed that the interaction between Al_2O_3 and TiO_2 hinders the phase transition of TiO_2 from amorphous to anatase.[32,44,45]

The XRD patterns of 20NiO/5Al_2O_3-TiO_2/WO_3 calcined at 400 °C for 1.5 h as a function of WO_3 content are shown in Figure 4. WO_3 remained amorphous to X-ray diffraction up to 15 wt%, indicating good dispersion on the surface of

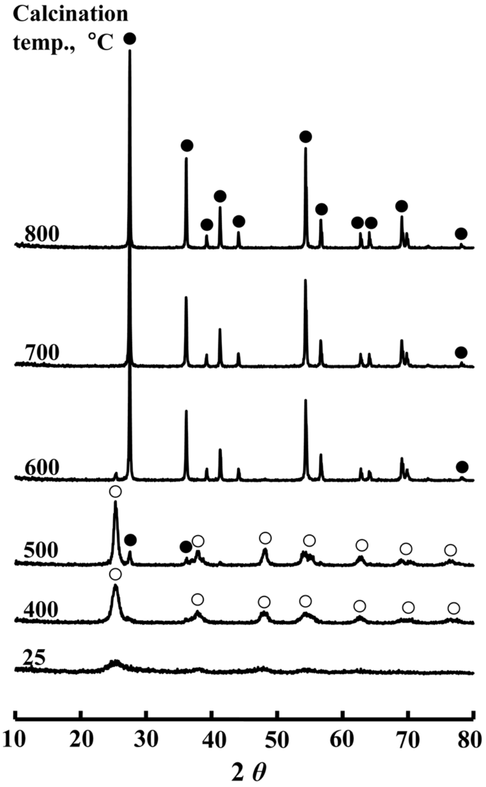

Figure 2. X-ray diffraction patterns of TiO_2 calcined at different temperatures for 1.5 h: (○), anatase phase of TiO_2; (●), rutile phase of TiO_2.

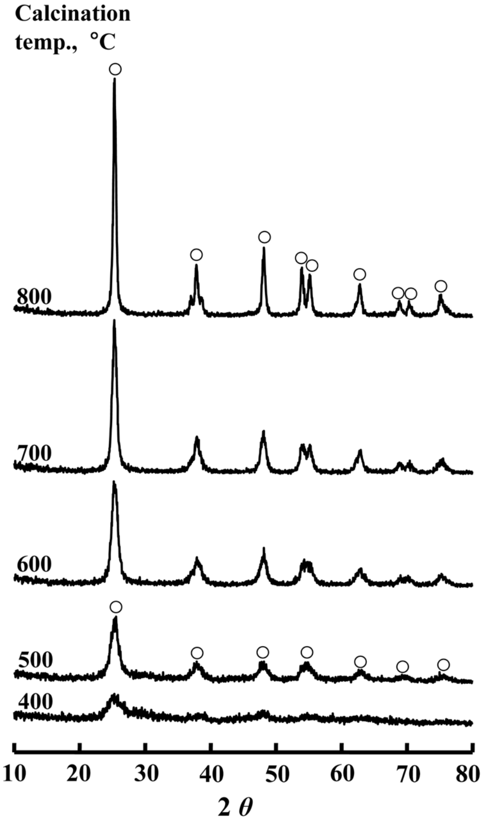

Figure 3. X-ray diffraction patterns of $5Al_2O_3$-TiO_2 calcined at different temperatures for 1.5 h: (○), anatase phase of TiO_2.

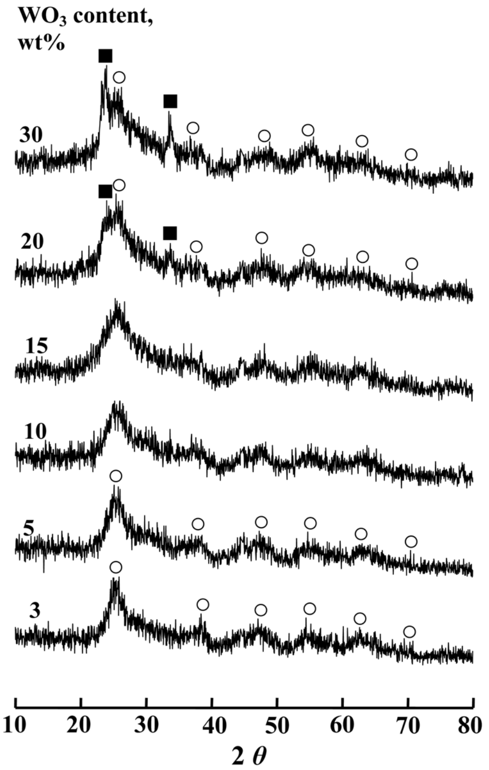

Figure 4. X-ray diffraction patterns of $20NiO/5Al_2O_3$-TiO_2/WO_3 containing different WO_3 contents and calcined at 400 °C for 1.5 h: (○), anatase phase of TiO_2; (■), monoclinic phase of WO_3.

catalyst. However, from 20 wt% of WO_3, the XRD data indicated the presence of a two-phase mixture of monoclinic phase of WO_3 and anatase phase of TiO_2, where the crystallinity of anatase phase TiO_2 was very poor due to the interaction between TiO_2 and the other oxides. In general, for the calcination temperature of 400-500 °C the hexagonal and monoclinic phases of WO_3 are present.[46] However, in case of $20NiO/Al_2O_3$-TiO_2/WO_3 containing WO_3 content above 15 wt%, only the monoclinic phase of WO_3 was observed, as shown in Figure 4.

NiO was amorphous to X-ray diffraction regardless of NiO content up to 30 wt% of NiO, indicating excellent dispersion on the surface of catalyst. For the above Al_2O_3-promoted catalysts, there are no characteristic peaks of Al_2O_3 in the XRD patterns, implying that Al_2O_3 is sufficiently homogeneously mixed with titania.

The crystalline structures of $20NiO/5Al_2O_3$-$TiO_2/15WO_3$ calcined in air at different temperatures for 1.5 h were examined. As shown in Figure 5, the catalyst was amorphous to X-ray diffraction up to 400 °C. However, for the calcination temperature of 500 °C XRD data indicated a two-phase mixture of monoclinic phase of WO_3 and anatase phase of TiO_2. The amount of two phases of TiO_2 and WO_3 increased with increasing calcination temperature, indicating that the interaction between NiO or WO_3 and TiO_2 hinders the transition of TiO_2 from amorphous to anatase phase.[44,47] The presence of NiO and WO_3 strongly influences the development of textural properties with temperature in

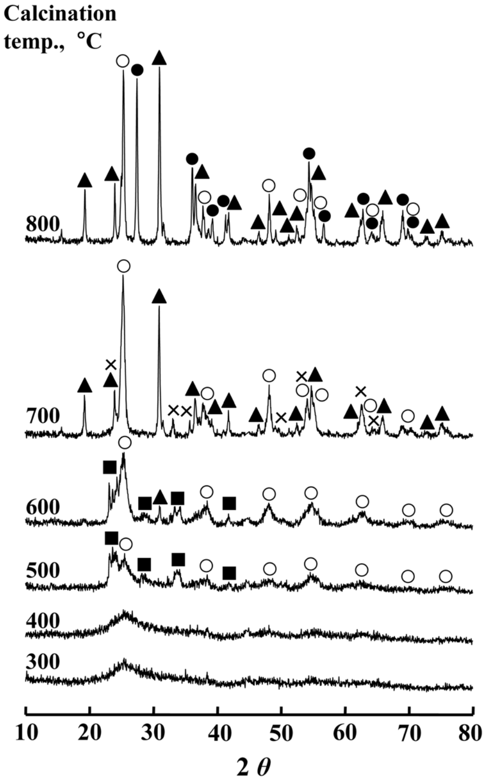

Figure 5. X-ray diffraction patterns of $20NiO/5Al_2O_3$-$TiO_2/15WO_3$ calcined at different temperatures for 1.5 h: (○), anatase phase of TiO_2; (●), rutile phase of TiO_2; (■), monoclinic phase of WO_3; (▲), monoclinic phase of $NiWO_4$; (×), rhombohedral phase of $NiTiO_3$.

comparison with pure TiO_2. In fact, it is reported that for pure TiO_2 two phases of anatase and rutile TiO_2 are present at the calcination temperature of 350 °C because of no interaction of titania.[47] No phase of NiO was observed in any phase at all calcination temperature, indicating good dispersion of NiO on the surface of TiO_2 support due to the interaction between them. For the calcination temperature of 600 °C a new phase of monoclinic nickel tungstate ($NiWO_4$) was observed through the reaction between NiO and WO_3, showing that the amount of nickel tungstate increased with increasing calcination temperature, as shown in Figure 5. For the calcination temperature of 700 °C a phase of rhombohedral nickel titanate ($NiTiO_3$) was observed newly through the reaction between NiO and TiO_2, but this phase disappeared at the calcination temperature of 800 °C due to the the decomposition of $NiTiO_3$. For the calcination temperature of 800 °C a phase transition from anatase TiO_2 to rutile TiO_2 occurred, showing the presence of a three-phase mixture of the anatase and rutile forms, and nickel tungstate.

Surface properties. The specific surface areas of $20NiO/5Al_2O_3$-TiO_2/WO_3 catalysts containing different WO_3 contents and calcined at 400 °C for 1.5 h are listed in Table 1. The presence of WO_3 also influences the surface area. The surface area increases gradually with increasing tungsten oxide loading up to 15 wt%. It seems likely that the interactions between tungsten oxide (or Al_2O_3) and TiO_2 prevent catalysts from crystallizing.[33] The decrease of surface area for $20NiO/5Al_2O_3$-TiO_2/WO_3 samples containing WO_3 above 15 wt % is also due to the blocking of TiO_2 pores by the increased WO_3 loading. The acidity of catalysts calcined at 400 °C, as determined by the amount of NH_3 irreversibly adsorbed at 230 °C,[37-39,44,48] is also listed in Table 1. It seems likely that strong acid sites are formed through the bonding between dispersed WO_3 and TiO_2. Similary to the case of sulfated metal oxides, the new acid sites can be formed and the acid strength can be strongly enhanced by the inductive effect of tungstate ion bonded to the surface of catalyst.[33,49]

Table 1. Specific surface area and acidity of 20-$NiO/5Al_2O_3$-TiO_2/WO_3 catalysts containing various WO_3 contents and calcined at 400 °C for 1.5 h

WO_3 content, wt%	Surface area, m^2/g	Acidity, μmol/g
0	200	192
3	257	210
5	262	213
10	269	221
15	285	247
20	236	226
30	226	220

We examined the effect of Al_2O_3 addition on the surface area and acidity of $20NiO/Al_2O_3$-$TiO_2/15WO_3$ samples. The specific surface areas and acidity of $20NiO/Al_2O_3$-$TiO_2/15WO_3$ catalysts containing different Al_2O_3 contents and calcined at 400 °C are listed in Table 2. Both surface area and acidity increased with increasing Al_2O_3 content up to 5 mol%, indicating the promoting effect of Al_2O_3 on the catalytic activity for ethylene dimerization described later.

The specific surface areas of $NiO/5Al_2O_3$-$TiO_2/15WO_3$ catalysts containing different NiO contents and calcined at 400 °C for 1.5 h were examined. The presence of NiO influences the surface area in comparison with that of the pure TiO_2. Specific surface areas of $5NiO/5Al_2O_3$-$TiO_2/15WO_3$ (260 m^2g^{-1}) and $20NiO/5Al_2O_3$-$TiO_2/15WO_3$ (285 m^2g^{-1}) samples are larger than that of $5Al_2O_3$-TiO_2 (93 m^2g^{-1}) calcined at the same temperature, showing that surface area increases gradually with increasing nickel oxide loading up to 20 wt%. It seems likely that the interactions between nickel oxide and TiO_2 prevent catalysts from crystallizing.[33] The decrease of surface area for $NiO/5Al_2O_3$-$TiO_2/15WO_3$ samples containing NiO above 20 wt % is also

Table 2. Specific surface area and acidity of 20-NiO/Al_2O_3-$TiO_2/15WO_3$ catalysts containing various Al_2O_3 contents and calcined at 400 °C for 1.5 h

Al_2O_3 content, mol %	Surface area, m^2/g	Acidity, μmol/g
0	172	182
1	193	193
2	240	230
3	250	241
5	285	247
7	269	184
10	234	161

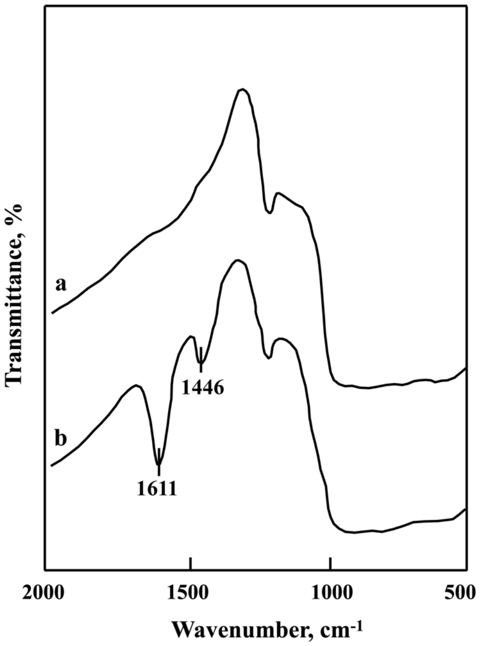

Figure 6. Infrared spectra of NH_3 adsorbed on 20NiO/5Al_2O_3-TiO_2/15WO_3: (a) background of 20NiO/5Al_2O_3-TiO_2/15WO_3 after evacuation at 400 °C for 1 h, (b) NH_3 adsorbed on (a), where gas was evacuated at 230 °C for 1 h.

due to the blocking of TiO_2 pores by the increased NiO loading.

Infrared spectroscopic studies of ammonia adsorbed on solid surfaces have made it possible to distinguish between Brönsted and Lewis acid sites.[50-52] Figure 6 shows the infrared spectra of ammonia adsorbed on 20NiO/5Al_2O_3-TiO_2/15WO_3 catalyst evacuated at 400 °C for 1 h. For 20NiO/5Al_2O_3-TiO_2/15WO_3, the band at 1446 cm^{-1} is the characteristic peak of ammonium ion, which is formed on the Brönsted acid sites. The absorption peak at 1611 cm^{-1} is contributed by ammonia coordinately bonded to Lewis acid sites,[50-52] indicating the presence of both Brönsted and Lewis acid sites on the surface of 20NiO/5Al_2O_3-TiO_2/15WO_3 catalyst. Other samples having different NiO and WO_3 contents also showed the presence of both Lewis and Brönsted acids.

Catalytic activities for ethylene dimerization

Effect of calcination temperature on catalytic activity. The catalytic activities of 20NiO/5Al_2O_3-TiO_2/15WO_3 were tested as a function of calcination temperature. The results are shown in Figure 7, where catalysts were evacuated at 400 °C for 1 h. The activities increased with the calcination temperature, reaching a maximum at 400 °C, and then the activities decreased. The decrease of catalytic activity after calcination above 400 °C can be attributed to the fact that the surface area and acidity above 400 ^{o}C decrease with the calcination temperature. As shown in Figure 5, for the calcination temperature above 400 ^{o}C various crystalline materials such as tungsten oxide, nickel titanate, nickel tungstate, and titania were formed and consequently the decrease of surface area and acidity gives rise to the decrease of catalytic activity. Thus, in our following experiments we placed emphsis on the catalysts calcined at 400 ^{o}C.

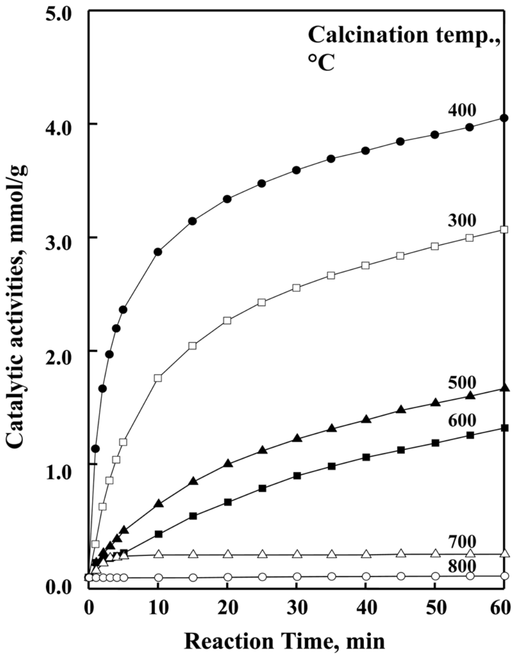

Figure 7. Catalytic activity of 20NiO/5Al_2O_3-TiO_2/15WO_3 at 20 °C as a function of calcination temperature.

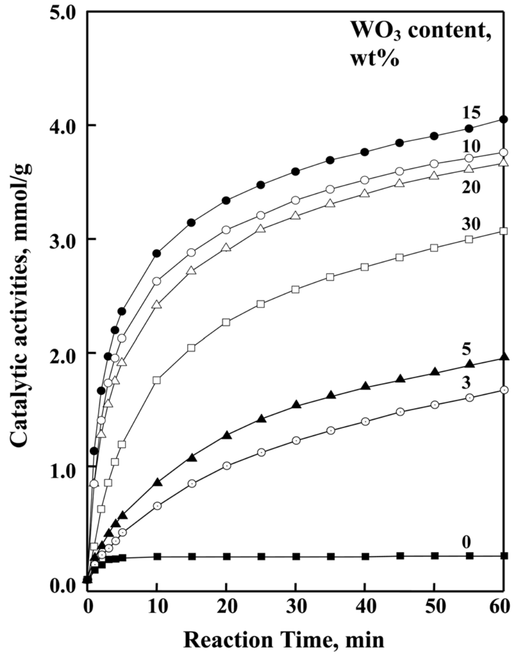

Figure 8. Catalytic activity of 20NiO/5Al_2O_3-TiO_2/WO_3 at 20 °C as a function of WO_3 content.

It was found that over 20NiO/5Al_2O_3-TiO_2/15WO_3, ethylene was continuously consumed, as shown by the results presented in Figure 7. Over all catalysts, ethylene was selectively dimerized to *n*-butenes. However, a small amount of hexenes from the phase adsorbed on the catalyst surface was detected. In the composition of *n*-butenes analyzed by gas chromatography, 1-butene was found to predominate ex-

Table 3. Dispersed WO_3 amount, specific surface area, acidity, and catalytic activity for ethylene dimerizaiton of $20NiO/5Al_2O_3$-TiO_2/WO_3 containing different WO_3 contents

Catalyst	Dispersed WO_3 amount [WO_3(g)/$20NiO/5Al_2lO_3$-TiO_2(g)]	Surface area, m^2/g	Acidity, μmol/g	Catalytic activity, mmol/g
$20NiO/5Al_2O_3$-$TiO_2/0WO_3$	0	200	192	0.2
$20NiO/5Al_2O_3$-$TiO_2/3WO_3$	0.03	257	210	0.4
$20NiO/5Al_2O_3$-$TiO_2/5WO_3$	0.05	267	213	0.7
$20NiO/5Al_2O_3$-$TiO_2/10WO_3$	0.11	269	221	2.1
$20NiO/5Al_2O_3$-$TiO_2/15WO_3$	0.18	285	247	2.3

clusively at the initial reaction time, as compared with *cis*-butene and *trans*-butene. This is because the initial product of ethylene dimerization is 1-butene.[4,9,50] Therefore, the initially produced 1-butene is also isomerized to 2-butene during the reaction time.[18,19,50,51]

Effect of WO_3 modification on catalytic activity. Recently, it has been reported that metal oxide modified with WO_3 can be used as an alternative catalyst in reactions requiring strong acid sites.[34] Several advantages of tungstate over sulfate as dopant include that it does not suffer from dopant loss during thermal treatment and it undergoes significantly less deactivation during catalytic reaction.

The catalytic activity of $20NiO/5Al_2O_3$-TiO_2/WO_3 as a function of WO_3 content is plotted in Figure 8. As shown in Figure 8, the maximum activity is obtained with the catalyst of 15 wt% WO_3, where the amount of dispersed WO_3 is maximum, as listed in Table 3. Therefore, it seems likely that the highest activity of the catalyst containing 15 wt% WO_3 is related to its acidity and acid strength. The high acid strength and acidity are responsible for the W=O bond nature of complex formed by the interaction between WO_3 and TiO_2.[34,53] As discussed in IR spectra, IR spectra of $20NiO/5Al_2O_3$-$TiO_2/15WO_3$ catalyst after evacuation at 400 °C showed the band at 1012 cm^{-1} due to the W=O stretching mode of the tungsten oxide complex bonded to the TiO_2 surface.[54] This isolated tungsten oxide species is stabilized through multiple W-O-Ti bonds between each WO_3 species and the TiO_2 surface.[55,56] As listed in Table 1, the acidity of $20NiO/5Al_2O_3$-$TiO_2/15WO_3$ catalyst is the most among the catalysts. Of course, the acidity of catalysts is related to their specific surface area, as mentioned above. In fact, Table 1 show that the specific surface area attained a maximum when the WO_3 content in $20NiO/5Al_2O_3$-TiO_2/WO_3 catalysts is 15 wt%.

The forms of active components present in heterogeneous catalysts are of importance to catalysis. A great many oxides can disperse spontaneously onto the surfaces of supports to form a monolayer, because the monolayer is a thermodynamically stable form.[57] When the loading amounts of WO_3 are low, the highly dispersed tungsten oxide species can not be detected by XRD, as shown in Figure 4. Therefore, we can estimate the states of dispersed WO_3 by the XRD analysis. Dispersed WO_3 amount, surface area, acid amount, and catalytic activity for $20NiO/5Al_2O_3$-TiO_2/WO_3 catalysts containing different WO_3 contents below 20 wt% are listed in Table 3. There are good correlations among the dispersed WO_3 amount, acidity, and catalytic activity. Namely, the larger the dispersed WO_3 amount, the higher both the acidity and the catalytic activity. This can be explained by the suggestion that strong acid sites are formed through the bonding between dispersed WO_3 and TiO_2 and consequently catalytic activity increases due to the increased acid sites.

The acid strength of the catalysts was examined by a color change method, using Hammett indicator[32,39] in sulphuryl chloride. The $5NiO/5Al_2O_3$-$TiO_2/15WO_3$ sample after enacuation at 500 °C for 1 h was estimated to have $H_0 \leq -14.5$, indicating the formation of superacidic sites. Acids stronger than $H_0 \leq -11.93$, which corresponds to the acid strength of 100% H_2SO_4, are superacids.[58] Consequently, NiO/Al_2O_3-TiO_2/WO_3 catalysts would be solid superacids. The superacidic property is attributed to the double bond nature of the W=O in the complex formed by the interaction of TiO_2 with tungstate, in analogy with the case of ZrO_2 modified with chromate and sulfate ions.[18,59]

Effect of Al_2O_3 addition on catalytic activity. The catalytic activity of $20NiO/Al_2O_3$-$TiO_2/15WO_3$ as a function of Al_2O_3 content for ethylene dimerization was examined,

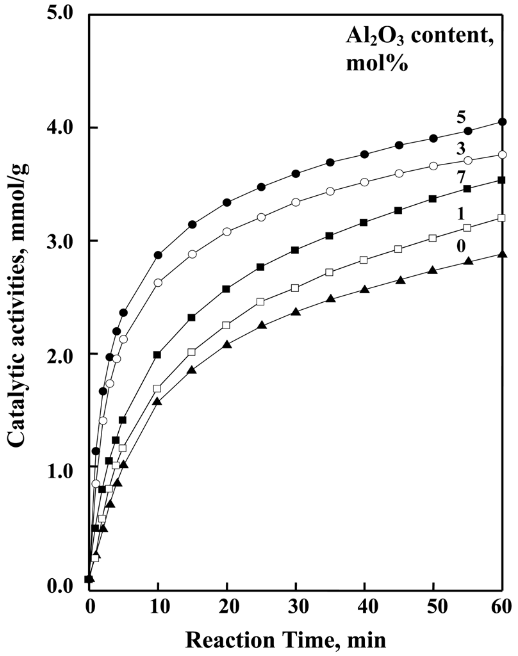

Figure 9. Catalytic activity of $20NiO/Al_2O_3$-$TiO_2/15WO_3$ at 20 °C as a function of Al_2O_3 content.

where the catalysts were pretreated at 400 °C for 1 h before reaction; the results are shown in the Figure 9. The catalytic activity increased with increasing the Al_2O_3 content, reaching a maximum at 5 mol%.

Considering the experimental results of Table 2 and Figure 9, it seems likely that the catalytic activity closely relates to the change of acidity of catalysts. As listed in Table 3, the total acid sites of $20NiO/5Al_2O_3$-$TiO_2/15WO_3$ and $20NiO/TiO_2/15WO_3$ are 247 μmol/g and 182 μmol/g, respectively, showing that the number of acid sites for the catalyst promoted with Al_2O_3 is greater than that for nonpromoted catalyst. This is consistent with the results reported by Hua *et al*. over Al_2O_3-promoted SO_4^{2-}/ZrO_2.[45] Al_2O_3-promoted catalysts could be related to a strong interaction between Al_2O_3 and TiO_2. Since the promoting effect of Al_2O_3 is related to an increase in number of surface acidic sites, it would be of interest to examine various factors influencing the enhancement of these surface acidic sites.

Xia *et al.*[60] proposed that Al_2O_3 incorporation in TiO_2 matrix brought about an increase of the positive partial charge on the Ti cations as a result of the formation of Al-O-Ti bonds which helped to stabilize the sulfate species at the oxide surface. The formation of Al-O-Ti bond on the surface of the Al_2O_3-promoted catalysts is probably the cause for the increase in strong acidic sites. According to the principle of electronegativity equalization proposed by Sanderson,[61] since the electronegativity of Al^{3+} is larger than that of Ti^{4+}, the positive charge on Ti atom is increased as a result of the formation of Al-O-Ti bond, which generates stronger acidity on these sites.[45] At the same time, the stronger Al-O-Ti bond formed by the charge transfer from Ti atom to neighboring Al atom results in an increase in the thermal stability of the surface tungstate species and consequently the acidity of Al_2O_3-promoted catalyst is increased.

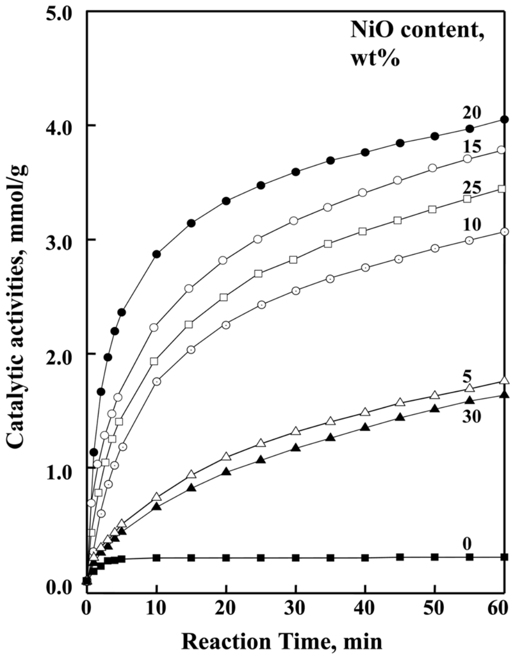

Figure 10. Catalytic activity of $NiO/5Al_2O_3$-$TiO_2/15WO_3$ at 20 °C as a function of NiO content.

Catalytic activity as a function of NiO content. The catalytic activity of $NiO/5Al_2O_3$-$TiO_2/15WO_3$ containing different NiO contents was examined; the results are shown as a function of NiO content in Figure 10. Catalysts were evacuated at 400 °C for 1 h before each reaction. The catalytic activity gives a maximum at 20 wt % of NiO. This seems to be correlated to the specific surface area and to the acidity of catalysts. The acidity of $NiO/5Al_2O_3$-$TiO_2/15WO_3$ calcined at 400 °C was determined by the amount of NH_3 irreversibly adsorbed at 230 °C.[37-39] As mentioned above, the BET surface area attained a maximum extent when the NiO content in the catalyst was 20 wt % and then showed a gradual decrease with increasing NiO content due to the blocking of TiO_2 pore by the increased NiO loading. It has been suggested that the active site for dimerization is formed by an interaction of a low-valent nickel ion with an acid site.[9,13] Therefore, as shown in Figure 10, $5Al_2O_3$-$TiO_2/15WO_3$ without NiO did not exhibit catalytic activity for ethylene dimerization absolutely. In fact, nickel oxide, which is active for C_2H_4-C_2D_4 equilibration, acquires an activity for ethylene dimerization upon addition of nickel sulfate, which is known to be an acid.[14] The presence of NiO may attract reactants and enhance the local concentration of reactants near acid sites,[48] consequently showing the increased catalytic activity. In view of Table 1 and Figure 10, the higher the acidity, the higher the catalytic activity. Good correlations have been found in many cases between the acidity and the catalytic activities of solid acids. For example, the rates of both the catalytic decomposition of cumene and the polymerization of propylene over SiO_2-Al_2O_3 and supported NiO catalysts were found to increase with increasing acid amount at strength $H_o \leq +3.3$.[62] The catalytic activity of nickel-containing catalysts in ethylene dimerization as well as in butene isomerization is closely correlated with the acidity of the catalyst.[4,8,46,53]

Conclusions

Strong solid acid catalysts, NiO/Al_2O_3-TiO_2/WO_3 were prepared by adding Al_2O_3 to TiO_2 and modifying TiO_2 with WO_3 for ethylene dimerization. $20NiO/5Al_2O_3$-$TiO_2/15WO_3$ containing 20 wt % NiO, 15 wt% WO_3 and 5 mol % Al_2O_3, and calcined at 400 °C, exhibited maximum catalytic activiy for ethylene dimerization. The strong acid sites were by the inductive effect of WO_3 species formed through the bonding between dispersed WO_3 and TiO_2. The larger the dispersed WO_3 amount, the higher both the acidity and catalytic activity. The addition of Al_2O_3 up to 5 mol% enhanced acidity and catalytic activity of NiO/Al_2O_3-TiO_2/WO_3 gradually due to the interaction between Al_2O_3 and TiO_2 and consequent formation of Al-O-Ti bond.

Acknowledgements. This work was supported by 2007 Research Fund of University of Ulsan. We wish to thank Korea Basic Science Institute (Daegu Branch) for the use of their X-ray diffractometer.

References

1. Pae, Y. I.; Lee, S. H.; Sohn, J. R. *Catal. Lett.* **2005**, *99*, 241.
2. Bernardi, F.; Bottoni, A.; Rossi, I. *J. Am. Chem. Soc.* **1998**, *120*, 7770.
3. Sohn, J. R.; Ozaki, A. *J. Catal.* **1979**, *59*, 303.
4. Sohn, J. R.; Ozaki, A. *J. Catal.* **1980**, *61*, 29.
5. Wendt, G.; Fritsch, E.; Schöllner, R.; Siegel, H. Z. *Anorg. Allg. Chem.* **1980**, *467*, 51.
6. Sohn, J. R.; Shin, D. C. *J. Catal.* **1996**, *160*, 314.
7. Berndt, G. F.; Thomson, S. J.; Webb, G. J. *J. Chem. Soc. Faraday Trans.* **1983**, *179*, 195.
8. Sohn, J. R.; Lim, J. S. *Bull. Korean Chem. Soc.* **2005**, *26*, 1029.
9. Sohn, J. R.; Park, W. C.; Kim, H. W. *J. Catal.* **2002**, *209*, 69.
10. Sohn, J. R.; Park, W. C. *Bull. Korean Chem. Soc.* **2000**, *21*, 1063.
11. Urabe, K.; Koga, M.; Izumi, Y. *J. Chem. Soc., Chem. Commun.* **1989**, 807.
12. Wendt, G.; Hentschel, D.; Finster, J.; Schöllner, R. *J. Chem. Soc. Faraday Trans.* **1983**, *179*, 2013.
13. Kimura, K.; Ozaki, A. *J. Catal.* **1964**, *3*, 395.
14. Maruya, K.; Ozaki, A. *Bull. Chem. Soc. Jpn.* **1973**, *46*, 351.
15. Hartmann, M.; Pöppl, A.; Kevan, L. *J. Phys. Chem.* **1996**, *100*, 9906.
16. Elev, I. V.; Shelimov, B. N.; Kazansky, V. B. *J. Catal.* **1984**, *89*, 470.
17. Choo, H.; Kevan, L. *J. Phys. Chem. B* **2001**, *105*, 6353.
18. Sohn, J. R.; Kim, H. J. *J. Catal.* **1986**, *101*, 428.
19. Sohn, J. R.; Lee, S. Y. *Appl. Catal. A: Gen.* **1997**, *164*, 127.
20. Sohn, J. R.; Kim, H. W.; Park, M. Y.; Park, E. H.; Kim, J. T.; Park, S. E. *Appl. Catal.* **1995**, *128*, 127.
21. Hsu, C. Y.; Heimbuch, C. R.; Armes, C. T.; Gates, B. C. *J. Chem. Soc., Chem. Commun.* **1992**, 1645.
22. Cheung, T. K.; Gates, B. C. *J. Catal.* **1997**, *168*, 522.
23. Adeeva, V.; de Haan, H. W.; Janchen, J.; Lei, G. D.; Schunemann, V.; van de Ven, L. J. M.; Sachtler, W. M. H.; van Santen, R. A. *J. Catal.* **1995**, *151*, 364.
24. Wan, K. T.; Khouw, C. B.; Davis, M. E. *J. Catal.* **1996**, *158*, 311.
25. Song, X.; Reddy, K. R.; Sayari, A. *J. Catal.* **1996**, *161*, 206.
26. Coelho, M. A.; Resasco, D. E.; Sikabwe, E. C.; White, R. L. *Catal. Lett.* **1995**, *32*, 253.
27. Hosoi, T.; Shimadzu, T.; Ito, S.; Baba, S.; Takaoka, H.; Imai, T.; Yokoyama, N. *Prepr. Symp. Div. Petr. Chem.*; American Chemical Society: Los Angeles, CA, 1988; p 562.
28. Ebitani, K.; Konishi, J.; Hattori, H. *J. Catal.* **1991**, *130*, 257.
29. Signoretto, M.; Pinna, F.; Strukul, G.; Chies, P.; Cerrato, G.; Ciero, S. D.; Morterra, C. *J. Catal.* **1997**, *167*, 522.
30. Hua, W.; Xia, Y.; Yue, Y.; Gao, Z. *J. Catal.* **2000**, *196*, 104.
31. Moreno, J. A.; Poncelet, G. *J. Catal.* **2001**, *203*, 153.
32. Sohn, J. R.; Cho, E. S. *Appl. Catal. A: Gen.* **2005**, *282*, 147.
33. Sohn, J. R. *J. Ind. Eng. Chem.* **2004**, *10*, 1.
34. Arata, K. *Adv. Catal.* **1990**, *37*, 165.
35. Hino, M.; Arata, K. *J. Chem. Soc., Chem. Commun.* **1987**, 1259.
36. Larsen, G.; Lotero, E.; Para, R. D. In *Proceedings of the 11th International Congress on Catalysis*; Elsevier: New York, 1996; p 543.
37. Sohn, J. R.; Lee, S. G.; Shin, D. C. *Bull. Korean Chem. Soc.* **2006**, *27*, 1623.
38. Sohn, J. R.; Shin, D. C.; Kim, H. W. *J. Ind. Eng. Chem.* **2007**, *13*, 47.
39. Sohn, J. R.; Kwon, S. H.; Shin, D. C. *Appl. Catal. A: Gen.* **2007**, *317*, 216.
40. Sohn, J. R.; Park, M. Y. *Langmuir* **1998**, *14*, 6140.
41. Vuurman, M. A.; Wachs, I. E.; Hirt, A. M. *J. Phys. Chem.* **1991**, *95*, 9928.
42. Cerrato, G.; Marchesea, L.; Marchesea, C. *Appl. Surf. Sci.* **1993**, *70*, 200.
43. Alemany, L. J.; Berti, F.; Busca, G.; Ramis, G.; Robba, D.; Toledo, G. P.; Trombetta, M. *Appl. Catal. B: Environ*. **1996**, *10*, 299.
44. Sohn, J. R.; Cho, S. G.; Pae, Y. I.; Hayashi, S. *J. Catal.* **1996**, *159*, 170.
45. Hua, W.; Xia, Y.; Yue, Y.; Gao, Z. *J. Catal.* **2000**, *196*, 104.
46. Sohn, J. R.; Han, J. S.; Kim, H. W.; Pae, Y. I. *Bull. Korean Chem. Soc.* **2005**, *26*, 755.
47. Sohn, J. R.; Lim, J. S. *Catal. Lett*. **2006**, *108*, 71.
48. Sohn, J. R.; Choi, H. D.; Shin, D. C. *Bull. Korean Chem. Soc.* **2006**, *27*, 821.
49. Tanabe, K.; Misono, M.; Ono, Y.; Hattori, H. *New Solid Acids and Bases*; Kodansha-Elsevier: Tokyo, 1989; p 185.
50. Sohn, J. R.; Lee, S. H. *Appl. Catal. A: Gen.* **2004**, *266*, 89.
51. Sohn, J. R.; Park, W. C. *Appl. Catal. A: Gen.* **2003**, *239*, 269.
52. Satsuma, A.; Hattori, A.; Mizutani, K.; Furuta, A.; Miyamoto, A.; Hattori, T.; Murakami, Y. *J. Phys. Chem.* **1988**, *92*, 6052.
53. Sohn, J. R.; Han, J. S. *Appl. Catal. A: Gen.* **2006**, *298*, 168.
54. Litteti, L.; Nova, I.; Ramis, G.; DallAcqua, L.; Busca, G.; Giamello, E.; Forzatti, P.; Bregani, F. *J. Catal.* **1999**, *187*, 419.
55. Liu, Z.; Chen, Y. *J. Catal.* **1998**, *177*, 314.
56. Zhao, B.; Wang, X.; Ma, H.; Tang, Y. *J. Mol. Catal. A: Chem.* **1996**, *108*, 167.
57. Xie, Y. C.; Tang, Y. Q. *Adv. Catal.* **1990**, *37*, 1.
58. Olah, F. G. A.; Prakash, G. K. S.; Sommer, J. *Science* **1979**, *206*, 13.
59. Sohn, J. R.; Ryu, S. G. *Langmuir* **1993**, *9*, 126.
60. Xia, Y.; Hua, W.; Gao, Z. *Appl. Catal. A: Gen.* **1999**, *185*, 293.
61. Sanderson, R. T. *Chemical Bonds and Bond Energy*; Academic Press: New York, 1976; p 75.
62. Tanabe, K. *Solid Acids and Bases*; Kodansha: Tokyo, 1970; p 103.